HHS Public Access

Author manuscript

Neuron. Author manuscript; available in PMC 2016 March 04.

Published in final edited form as:

Neuron. 2015 March 4; 85(5): 1056–1069. doi:10.1016/j.neuron.2015.01.024.

RIM-Binding Protein Links Synaptic Homeostasis to the Stabilization and Replenishment of High Release Probability Vesicles

Martin Müller[1], **Özgür Genç**, and **Graeme W. Davis**[*]

Department of Biochemistry and Biophysics University of California, San Francisco San Francisco, CA 94158 USA

Abstract

Here we define activities of RIM-Binding Protein (RBP) that are essential for baseline neurotransmission and presynaptic homeostatic plasticity. At baseline, *rbp* mutants have a ~10-fold decrease in the apparent Ca^{2+} sensitivity of release that we attribute to 1) impaired presynaptic Ca^{2+} influx, 2) looser coupling of vesicles to Ca^{2+} influx and 3) limited access to the readily-releasable vesicle pool (RRP). During homeostatic plasticity, RBP is necessary for the potentiation of Ca^{2+} influx and the expansion of the RRP. Remarkably, *rbp* mutants also reveal a rate-limiting stage required for the replenishment of high-release probability (p) vesicles following vesicle depletion. This rate slows ~4-fold at baseline and nearly 7-fold during homeostatic signaling in *rbp*. These effects are independent of altered Ca^{2+} influx and RRP size. We propose that RBP stabilizes synaptic efficacy and homeostatic plasticity through coordinated control of presynaptic Ca^{2+} influx and the dynamics of a high-p vesicle pool.

INTRODUCTION

Homeostatic signaling systems stabilize the active properties of nerve and muscle cells (Davis, 2006; Marder, 2011; Turrigiano, 2011; Davis, 2013). The homeostatic modulation of presynaptic neurotransmitter release, referred to here as ‘presynaptic homeostasis’, is an evolutionarily conserved form of homeostatic plasticity that has been documented at neuromuscular junctions (NMJ) in systems ranging from *Drosophila* to human (Davis, 2013; Plomp et al., 1992). There is also evidence for presynaptic homeostasis at synapses throughout the mammalian central nervous system (Burrone et al., 2002; Kim and Ryan, 2010; Thiagarajan et al., 2005; Zhao et al., 2011). At the NMJ, inhibition of postsynaptic neurotransmitter receptors elicits an increase in presynaptic release that precisely offsets the magnitude of receptor perturbation and, thereby, restores postsynaptic muscle depolarization to baseline. Remarkably, different magnitudes of postsynaptic receptor perturbation induce

[*]to whom correspondence should be addressed Graeme.davis@ucsf.edu.

[1]Current Address: Institute of Molecular Life Sciences, University of Zurich 8057 Zurich, Switzerland

different levels of presynaptic homeostatic compensation (Frank et al., 2006). Therefore, presynaptic homeostasis requires mechanisms that can accurately tune neurotransmitter release over a wide range and, then, stably maintain the newly established levels of presynaptic release.

Two presynaptic processes have been shown to be essential for presynaptic homeostasis: 1) modulation of presynaptic Ca^{2+} influx through the CaV2.1 Ca^{2+} channel (Frank et al., 2006; Müller and Davis, 2012) and 2) modulation of the readily-releasable pool of synaptic vesicles (RRP; Müller et al., 2012; Weyhersmüller et al., 2011). Recent evidence suggests that these processes are molecularly separable. The homeostatic modulation of presynaptic Ca^{2+} influx requires the expression of a presynaptic DEG/ENaC sodium leak channel (Younger et al., 2013), whereas homeostatic RRP modulation requires the presynaptic adaptor protein RIM (Rab3-Interacting Molecule; Müller et al., 2012). It remains unknown how the homeostatic modulation of Ca^{2+} influx and RRP size is coordinated, because molecules that participate in both processes have not been identified. Furthermore, it seems likely that additional presynaptic processes will be engaged during homeostatic plasticity in order to sustain potentiated release for prolonged periods of time. Yet, these additional processes and their mechanistic control remain unknown.

Here we make several advances, placing RIM-Binding Protein (RBP) at the forefront of presynaptic homeostatic plasticity. RBPs biochemically interact with two proteins that are central to presynaptic Ca^{2+} signaling and RRP modulation: Cav2.1 Ca^{2+} channels and RIM (Hibino et al., 2002; Liu et al., 2011). It was recently shown that RBP resides at the center of presynaptic active zones, where it surrounds presynaptic CaV2.1 Ca^{2+} channels (Liu et al., 2011). This previous study analyzed RBP's role in baseline synaptic transmission, finding that loss of RBP causes impaired Ca^{2+} channel clustering and impaired presynaptic Ca^{2+} influx with an associated deficit in neurotransmitter release (Liu et al., 2011).

We now demonstrate that RBP is essential for the homeostatic modulation of neurotransmitter release, being required for both the modulation of calcium influx and the RRP. As such, RBP is the first presynaptic protein that could reasonably participate in coordinating these two homeostatic changes. Then, we define another novel activity of RBP, demonstrating that RBP is essential for the normal resupply of high-release probability vesicles. We demonstrate that loss of *rbp* slows the resupply of high-release probability vesicles by ~400%. This change is an order of magnitude more pronounced than previously described for Ca^{2+}-dependent effects on the rate of vesicle resupply (Hallermann and Silver, 2013; Sakaba and Neher, 2001). Finally, we connect this new activity of RBP during vesicle resupply to the mechanisms of presynaptic homeostatic plasticity. In so doing, we provide evidence that presynaptic homeostasis acts primarily upon a pool of high-release probability vesicles that are thought to reside at the active zone in close proximity to presynaptic Ca^{2+} channels and RBP. We propose that RBP is a molecular keystone with actions that are uniquely important for the stabilization of baseline neurotransmission, coupling of vesicles to sites of Ca^{2+} influx, and the stable, persistent homeostatic modulation of presynaptic neurotransmitter release.

RESULTS

Homeostatic Potentiation of Neurotransmitter Release is Blocked in *rbp* Mutants

To test RBP function during homeostatic plasticity, we assayed the homeostatic modulation of presynaptic release in a recently described *Drosophila rbp* null mutation that eliminates RBP protein (‘*drbp*’, $drbp^{stop1}/drbp^{S2.01}$; Liu et al., 2011; henceforth called *rbp*; 1.5mM $[Ca^{2+}]_e$; Figure 1A). Application of sub-saturating concentrations of the glutamate receptor antagonist philanthotoxin-433 (‘PhTX’, 20 μM)to the NMJ for 10 minutes significantly reduced the amplitude of spontaneous miniature EPSPs (mEPSPs) in both wild-type (‘wt’) and *rbp* mutants (Figure 1C, left; $p<0.001$ for both wt and *rbp*). All average data and sample sizes are reported in figure legends and/or Table S1. At wild-type synapses, the decrease in mEPSP amplitude in the presence of PhTX is correlated with a significant increase in neurotransmitter release (‘quantal content’=EPSP amplitude/mEPSP amplitude; Figure 1B, top; 1C, right; $p<0.001$). Increased presynaptic release restores EPSP amplitudes to baseline values seen in the absence of PhTX (Figure 1C, middle; $p=0.28$). By contrast, *rbp* mutant synapses have impaired baseline release (Figure 1B, bottom; 1C, middle; note that current clamp recordings under-estimate this deficit, see below) and the homeostatic modulation of presynaptic release is completely absent, as shown by similar quantal content values for *rbp* in the absence and presence of PhTX (Figure 1B; 1C, right; $p=0.85$). As a consequence, EPSP amplitudes are significantly smaller in the presence of PhTX (Figure 1B; 1C, middle; $p<0.001$). These data indicate that RBP is necessary for synaptic homeostasis.

To confirm and extend the finding that RBP is necessary for synaptic homeostasis we repeated our analysis of presynaptic homeostasis, assaying release over a 15-fold range of extracellular Ca^{2+}, $[Ca^{2+}]_e$, using two-electrode voltage clamp to measure synaptic currents at a holding potential of −65mV. At wild-type synapses, EPSC amplitudes in the presence or absence of PhTX (20μM) were statistically similar between 0.3mM and 3mM $[Ca^{2+}]_e$ (Figure 1D, E, gray and black data; all $p \geq 0.84$). Remarkably, at 15mM $[Ca^{2+}]_e$ there was even a slight increase in EPSC amplitude upon PhTX application ($p=0.04$). Thus, robust homeostatic plasticity can be expressed over broad range of $[Ca^{2+}]_e$ at wild-type synapses. By contrast, when we examine homeostatic plasticity at different $[Ca^{2+}]_e$ in *rbp* mutants, we find that EPSC amplitudes are significantly smaller in the presence of PhTX at all $[Ca^{2+}]_e$ (Figure 1D, E, open red and filled red data; all $p \leq 0.02$). Since enhanced presynaptic Ca^{2+} influx, achieved by altering $[Ca^{2+}]_e$, does not restore homeostatic plasticity in *rbp* mutants, we conclude that the defect in homeostatic plasticity observed in *rbp* is unlikely to be a secondary consequence of impaired baseline neurotransmitter release or impaired baseline presynaptic Ca^{2+} influx.

The Homeostatic Enhancement of Presynaptic Ca^{2+} Influx Requires RBP

Synaptic homeostasis requires the potentiation of Ca^{2+} influx through presynaptic CaV2.1 Ca^{2+} channels (Frank et al., 2006; Müller and Davis, 2012). Because RBPs biochemically interact with presynaptic voltage-gated Ca^{2+} channels (Hibino et al., 2002; Liu et al., 2011), they are a candidate for participating in this process. To test this possibility we imaged presynaptic Ca^{2+} influx at baseline and following the induction of presynaptic homeostasis (see Experimental Procedures and Müller and Davis, 2012). First, we replicated the

previously reported finding that postsynaptic glutamate receptor perturbation induces a 23-30% increase in the peak amplitude of single action potential induced presynaptic Ca^{2+} transients (Müller and Davis, 2012). Here we find that the amplitude of presynaptic spatially averaged Ca^{2+} transients is significantly increased by 28% following application of PhTx to the NMJ (wt $\Delta F/F = 0.81 \pm 0.04$, N=22 and wt+PhTx $\Delta F/F = 1.04 \pm 0.07$, N=22, p=0.01). There was no difference in baseline Ca^{2+} indicator (OGB-1) loading (wt $F_{base} = 359 \pm 22$ and wt+PhTx $F_{base} = 351 \pm 30$; p=0.85). Next, in a separate set of experiments, we show that under baseline conditions, the peak amplitude of presynaptic spatially averaged Ca^{2+} transients in *rbp* mutants are significantly smaller than in wild-type controls (−28%; Figure 2A, B; p=0.049), consistent with a previous study (Liu et al., 2011). Then, we demonstrate that at *rbp* synapses, PhTX application fails to induce a significant increase in Ca^{2+} transient amplitude (Figure 2A, B; p=0.37). Again, there were no significant changes in baseline Ca^{2+} indicator fluorescence intensity or Ca^{2+} transient decay kinetics comparing the different groups and conditions (all p>0.65; Figure 2C), indicating that this phenotype is not due to differences in Ca^{2+}-indicator loading, Ca^{2+} buffering, and/or Ca^{2+} extrusion. Thus, loss of *rbp* completely blocks the homeostatic enhancement of presynaptic Ca^{2+} influx.

RBP controls access to the readily-releasable pool of synaptic vesicles

To examine how vesicles are functionally distributed relative to sites of Ca^{2+} influx, we assessed the effects of the Ca^{2+} chelator EGTA on synaptic transmission. EGTA has relatively slow Ca^{2+}-binding kinetics (Smith et al., 1984) and is, therefore, expected to primarily interfere with the release of vesicles that are either located at some distance from the sites of Ca^{2+} influx and/or have a lower Ca^{2+} affinity independent of their distance to Ca^{2+} channels. Thus, an increased sensitivity of release to EGTA is indicative of either an increased distance between Ca^{2+} channels and releasable vesicles or a steady-state difference between the contribution of high and low Ca^{2+} affinity vesicles. First, we probed the effects of EGTA-AM (25 μM for 10 min, see Experimental Procedures) on EPSCs evoked by motoneuron stimulation at two different stimulation frequencies (0.1 Hz, and 1 Hz) at 3mM $[Ca^{2+}]_e$. EGTA application reduced wild-type EPSC amplitudes by 12%, and 8% compared to controls stimulated at 0.1 Hz and 1 Hz, respectively (Figure 3A, B, gray data, '3 Ca'). In contrast, EGTA induced a much more pronounced drop in EPSC amplitude using the same experimental paradigm in *rbp* mutants (61% and 58% decrease at 0.1Hz and 1Hz, respectively; both p≤0.002 compared to wild type; Figure 3A, B, red data). The differential effects of EGTA comparing *rbp* and wild type could arise from differences in baseline Ca^{2+} influx. Therefore, we assayed EGTA sensitivity in wild-type animals after titrating $[Ca^{2+}]_e$ such that the average baseline EPSC amplitude in wild type was similar to *rbp* mutant EPSC amplitudes at 3mM $[Ca^{2+}]_e$. This equivalence point was reached at 0.45mM $[Ca^{2+}]_e$ (p=0.95). Remarkably, EGTA application to wild-type animals at 0.45mM $[Ca^{2+}]_e$ had a significantly smaller effect on EPSC amplitudes when compared to *rbp* mutants tested at 3mM $[Ca^{2+}]_e$ (Figure 3B, gray data, '0.45 Ca'; p=0.0003). Thus, the increased EGTA sensitivity in *rbp* mutants cannot be attributed to a difference in baseline Ca^{2+} influx or transmission. Taken together, these data suggest that there is a pronounced change in the population of release-ready vesicles. One possibility is that there is a shift from 'intrinsically' high to low Ca^{2+} affinity vesicles in *rbp*. Alternatively, there is an increased distance between Ca^{2+} channels and release-ready synaptic vesicles in *rbp*

mutants. This later possibility is consistent with recent electron microscopy data revealing a decrease in the number of vesicles located ≤ 5nm from the active-zone membrane at *rbp* mutant terminals (Liu et al., 2011). We conclude that loss of *rbp* not only impairs presynaptic Ca^{2+} influx, but also causes 'looser coupling' between the sites of Ca^{2+} influx and vesicles.

We next asked whether a reduction in the number of release-ready vesicles contributes to the deficit in baseline transmission in *rbp* mutants. To do so, we assessed the size of the readily-releasable vesicle pool (RRP) at different $[Ca^{2+}]_e$ by employing cumulative EPSC amplitude analysis during brief stimulus trains (Figure 3C, D, Müller et al., 2012; Schneggenburger et al., 1999; Weyhersmüller et al., 2011; see Experimental Procedures). First, we observed that cumulative EPSC amplitudes increased as a function of $[Ca^{2+}]_e$ at wild-type synapses, with a significant increase in cumulative EPSC amplitude between 0.4mM and 3mM $[Ca^{2+}]_e$ ($p=0.002$), and no significant change between 3mM and 15mM $[Ca^{2+}]_e$ (Figure 3D, black data ; $p=0.32$). This result suggests that changes in presynaptic Ca^{2+} influx alter neurotransmitter release in part by changing the apparent RRP size, consistent with data at a mammalian central synapse (Schneggenburger et al., 1999; Thanawala and Regehr, 2013). In *rbp* mutants, RRP size could not be estimated at 0.4mM $[Ca^{2+}]_e$ due to lack of synaptic depression (data not shown). The cumulative EPSC amplitude at 1mM $[Ca^{2+}]_e$ in *rbp* was still slightly smaller than the cumulative EPSC amplitude at 0.4mM $[Ca^{2+}]_e$ in wild type (Figure 3D, red and black data; $p=0.06$). Elevating $[Ca^{2+}]_e$ to 3 and 15mM $[Ca^{2+}]_e$ demonstrates a positive correlation between apparent RRP size and $[Ca^{2+}]_e$ in *rbp* mutants. However, there was still a significant reduction in cumulative EPSC amplitude in *rbp* at 3mM $[Ca^{2+}]_e$ as compared to wild-type controls ($p=0.04$), indicating a strong reduction in RRP size in *rbp* at physiological $[Ca^{2+}]_e$. Thus, the severe release defect seen in *rbp* at physiological $[Ca^{2+}]_e$ is caused, in part, by a reduction in the number of release-ready vesicles. Remarkably, when we increased $[Ca^{2+}]_e$ to very high levels (15mM, Figure 3C, D) cumulative EPSC amplitudes in *rbp* mutants were not significantly different compared to wild-type indicating that the absolute size of the RRP is unaffected by loss of RBP (Figure 3C, D; $p=0.19$). Based on these data, we conclude that RBP does not control total vesicle number in the RRP. Rather, RBP is required to efficiently access vesicles within the RRP.

There remains a significant deficit in presynaptic release in response to single action potential (AP) stimulation in *rbp* mutants at 15mM $[Ca^{2+}]_e$ (Figure 1D, E), even though RRP size is wild type (Figure 3D). This cannot be explained solely by a decrease in presynaptic calcium influx. Although Ca^{2+} influx is clearly diminished (−28%) in *rbp* compared to wild type at 1mM $[Ca^{2+}]_e$ (Figure 2), consistent with previously published data (Liu et al., 2011), we cannot resolve a difference in Ca^{2+} influx comparing *rbp* with wild type when recording at elevated $[Ca^{2+}]_e$ (3mM; see below). In this experiment, wild type and *rbp* had similar $\Delta F/F$ peak amplitudes (1.08 ± 0.18 vs. 1.29 ± 0.12, respectively; $p=0.3$), and there was no significant difference in baseline fluorescence ($p=0.26$), or decay kinetics of the calcium transient (not shown; see also below). We provide additional evidence that the Ca2+ indicator is not saturated under these recording conditions (Figure S1), further supporting the conclusion that the similar Ca2+ transient amplitudes at higher [Ca2+]e are not a consequence of dye loading or saturation. The absence of an apparent defect in Ca2+

influx in rbp at elevated [Ca2+]e is evidence that a decrease in Ca2+ influx cannot be the only cause underlying the release defect. Based on the substantially increased sensitivity of the *rbp* mutant to EGTA and the limited access to the RRP (Figure 3), we propose that the deficit in presynaptic release measured at elevated $[Ca^{2+}]_e$ is primarily due to looser coupling of vesicles to sites of Ca^{2+} influx. Three further observations are consistent with this interpretation. First, at 15mM $[Ca^{2+}]_e$, *rbp* mutants show almost no paired-pulse depression during 60-Hz stimulation, in striking contrast to pronounced depression observed in wild type (Figure 3E, left; $p<0.001$). Combined with the observation of no change in presynaptic Ca^{2+} influx between *rbp* and wild type at elevated $[Ca^{2+}]_e$, the difference in paired-pulse depression is likely due to a defect that is independent of Ca2+ influx. Second, single EPSCs recorded in *rbp* mutants rise more slowly than in wild type (Figure 3E, right; $p=0.02$), consistent with vesicles residing at a greater distance from sites of calcium entry. Third, we note a trend towards shallower slopes of the cumulative EPSC amplitude fits in *rbp* mutants (Figure 3C, 19.0±3.4 nA/stimulus; 15mM $[Ca^{2+}]_e$) compared to wild-type controls (29.2±4.4 nA/stimulus; $p=.0.072$; not shown), indicative of a decrease in steady-state release probability and/or a slower rate of vesicle replenishment.

Homeostatic Enhancement of the RRP is Blocked in *rbp*

Since the size of the RRP is similar in wild type and *rbp* mutants at 15mM $[Ca^{2+}]_e$ (Figure 3D), we are able to directly compare the homeostatic modulation of the RRP in these two genotypes at this Ca^{2+} concentration (Figure 4). PhTX application reduced mEPSP amplitude in both *rbp* and wild type (Figure 4B, left; both $p<0.001$), indicating that synapses of both genotypes were homeostatically challenged. At wild-type synapses, cumulative EPSC amplitudes were similar in the absence and presence of PhTX ($p=0.2$: Figure 4A, 4B, middle). The apparent RRP size is given by the ratio of the back-extrapolated cumulative EPSC amplitude and quantal size. The combination of a similar cumulative EPSC amplitude and a decrease in quantal size after PhTX application (Figure 4B, left, middle) translates into an increase in RRP size upon homeostatic challenge in wild-type animals (Figure 4B, right), consistent with previous findings (Müller et al., 2012; Weyhersmüller et al., 2011). In contrast, PhTX treatment leads to a significant decrease in cumulative EPSC amplitude in *rbp* mutants (Figure 4A, bottom, Figure 4B, middle; $p<0.001$). In fact, RRP modulation was not only blocked, but RRP size was significantly decreased upon PhTX application in *rbp* compared to baseline (Figure 4B, right; $p=0.003$). Thus, RBP is required for the homeostatic enhancement of RRP size and might be required to stabilize the RRP during homeostatic plasticity.

Two additional points are worth noting. First, it is remarkable that the RRP can be doubled during homeostatic plasticity at the wild type NMJ when recording at 15mM $[Ca^{2+}]_e$. Based on data presented in Figure 3, it appears that access to the RRP is saturated at this Ca^{2+} concentration and, yet, it is still possible to double the size of the RRP. This emphasizes that the homeostatic modulation of RRP is not simply due to a change in presynaptic Ca^{2+} influx and likely involves additional post-translational changes within the presynaptic nerve terminal that require RBP. We also note that RBP is the first molecule that is required for both the homeostatic enhancement of presynaptic Ca^{2+} influx (Figure 2) and the homeostatic

potentiation of RRP size (Figure 4). As such, RBP might coordinate these parallel processes during presynaptic homeostasis (see Discussion).

RBP is required for the replenishment of high-release probability vesicles

In principle, the size of the RRP could be increased by changing the number of vesicles that are partitioned between the reserve and readily-releasable pools. As such, the process of moving vesicles from the reserve to the RRP could be an important site of regulation during homeostatic plasticity. This process is commonly studied by measuring the rate of vesicle resupply to the RRP following a high-frequency stimulus train. At most synapses, vesicle resupply following a high-frequency stimulus train can be subdivided into two kinetic phases; 1) a fast recovery phase, which likely reflects the resupply of vesicles with relatively slow release kinetics/low release probability and 2) a slow recovery phase that likely corresponds to the replenishment of 'fast', 'high release probability' vesicles (Hallermann and Silver, 2013; Sakaba and Neher, 2001; Wu and Borst, 1999). Several synaptic proteins have been shown, through genetic loss of function studies, to primarily impair the *fast* recovery phase, and thus the resupply of 'low release probability' vesicles following AP stimulus trains (Frank et al., 2010; Hallermann et al., 2010a; 2010b). In these studies, the fast recovery component is slowed following disruption of calmodulin (Junge et al., 2004; Sakaba and Neher, 2001), Munc-13 (Junge et al., 2004; Lipstein et al., 2013), Bassoon (Frank et al., 2010; Hallermann et al., 2010b) and the C-terminus of Bruchpilot (Hallermann et al., 2010a). By contrast, the molecular mechanisms that control the resupply of high-release probability vesicles are largely unknown (Hallermann and Silver, 2013).

Here, synapses were stimulated with a brief 60-Hz train to measure baseline RRP size and to deplete the RRP. The first train was followed by a second 60-Hz train at various inter-train intervals ('ITI') to probe vesicle resupply/recovery from synaptic depression at high $[Ca^{2+}]_e$ (15mM) (Figure 5A). In wild-type animals, the recovery time course of the first EPSC amplitude of the second train (henceforth referred to as 'single EPSCs') was biphasic, with a fast kinetic phase (τ_{fast} =100±37 ms; Figure 5B, left; 5D), followed by a slow kinetic phase (τ_{slow}=5.8±1.8 s; Figure 5B, left; 5D), similar to previously published results (Hallermann et al., 2010a). In *rbp* mutants, the fast recovery phase had a similar time course (τ_{fast}=99±30 ms; Figure 5B, right; 5D) compared to wild-type (p=0.99). By contrast, the slow recovery component was drastically altered, being almost 400% slower in *rbp* compared to wild type (τ_{slow}= 20.9±1.8 s; p=0.004; Figure 5B, right; 5D). We did not detect significant differences in the relative amplitude of both kinetic components between wild type and *rbp* (p=0.61: with the slow kinetic component contributing 52% and 60% in wild type and *rbp*, respectively; not shown). Based on previous work, the fast recovery phase likely reflects the resupply of vesicles that are released with relatively low probability and slow kinetics, while the slow recovery phase likely corresponds to the replenishment of 'fast', 'high release probability' vesicles (Sakaba and Neher, 2001; Wu and Borst, 1999). RBP therefore appears to be a major molecular mechanism driving the resupply of fast, high release probability vesicles.

A similar result was obtained when analyzing the recovery time course of cumulative EPSC amplitudes, a proxy for RRP size (Figure 5D, right). The loss of *rbp* significantly slowed

both the fast and the slow phase of RRP recovery (τ_{fast}=479.5±124.5 ms, (τ_{slow}=10.4±2.7 s; Figure 5D, right) as compared to wild-type controls (τ_{fast}=137.2±52.4, τ_{slow}=2.2±0.3 s; Figure 5D; both $p<0.04$). Again, this result suggests that RBP is crucial for normal vesicle resupply dynamics.

It is well established that Ca^{2+} facilitates the rate of vesicle recovery (Hallermann and Silver, 2013). Therefore, we performed a series of experiments to control for the possibility that differences in vesicle recovery rates are a secondary consequence of diminished presynaptic Ca^{2+} influx in the *rbp* mutant. To do so, we chose to compare the rate of vesicle recovery in wild type at 3mM $[Ca^{2+}]_e$ (Figure 5E, '− PhTX') to the recovery rate in *rbp* recorded at 15mM $[Ca^{2+}]_e$ (Figure 5D, gray data). There are several justifications for this comparison: First, the average EPSC amplitude is statistically similar when comparing wild type at 3mM $[Ca^{2+}]_e$ to *rbp* mutants at 15mM $[Ca^{2+}]_e$ (indeed wt is slightly reduced, Figure 1E; $p<0.001$). Thus, we guarantee similar levels of absolute neurotransmitter release and, therefore, similar 'demands' upon the process of vesicle recovery. Second, while Ca^{2+} imaging data suggest that there is a negligible difference in Ca^{2+} influx when comparing wild type with *rbp* at 3mM $[Ca^{2+}]_e$, we can be certain that Ca^{2+} influx is not lower than in wild type when we compare *rbp* at 15mM $[Ca^{2+}]_e$ with wild type at 3mM $[Ca^{2+}]_e$. Finally, the fast and slow rates of vesicle recovery in wild type are not different at 3mM $[Ca^{2+}]_e$ and 15mM $[Ca^{2+}]_e$ (Figure 5D, E; light gray data; all $p\geq0.5$), further enabling a comparison of wild type at 3mM to *rbp* at 15mM $[Ca^{2+}]_e$. When we compare recovery rates between wild type at 3mM $[Ca^{2+}]_e$ (Figure 5E, '− PhTX') and *rbp* at 15mM $[Ca^{2+}]_e$ (Figure 5D, red data), we find that wild-type synapses recover substantially faster compared to *rbp* (τ_{slow}; $p=0.008$). We also note that the recovery of the cumulative EPSC is slower in *rbp* compared to wild type (Figure 5E; $p=0.04$). Thus, the elevation of intra-terminal Ca^{2+} during stimulus trains used to assess the cumulative EPSC did not restore the slow vesicle recovery seen in *rbp* to wild-type levels. These data argue that differences in intra-terminal Ca^{2+} cannot account for the defect in the rate of vesicle resupply observed in *rbp*.

Several additional experiments were performed to test whether the slow replenishment rates of *rbp* synapses are due to a defect in presynaptic Ca^{2+} influx. First, presynaptic Ca^{2+} influx in response to single-AP stimulation was directly assessed before and after a 60-Hz train (Figure 6). There is no difference in single AP induced Ca^{2+} influx, measured prior to the train (Figure 6A, B). Then, we measured presynaptic Ca^{2+} influx 5s after the stimulus train, a time point when the wild-type EPSC is ~70% recovered while the EPSC in *rbp* remains significantly smaller (~45% of control; Figure 6D). We demonstrate that there is no significant difference in presynaptic Ca^{2+} influx comparing wild type and *rbp* at the 5s time point (Figure 6A,B; $p=0.28$). We also assessed presynaptic Ca^{2+} during 60-Hz stimulation and don't observe differences between *rbp* and wild type (Figure S1). Thus, the relative difference in EPSC recovery between *rbp* and wild type at this interval cannot be explained by a defect in presynaptic Ca^{2+} influx.

Next, we probed EPSC recovery in *rim* mutants. The rational for this experiment is that *rim* mutants also block homeostatic plasticity and cause a 30% reduction in Ca^{2+} influx compared to wild type (Müller et al., 2012), very similar to that observed in *rbp*. If decreased presynaptic Ca^{2+} influx is the primary cause underlying the slow replenishment

rates of *rbp* synapses, then one expects to observe similarly slow replenishment rates in *rim*. However recovery from depression in *rim* is similar to wild type ($p>0.3$ at ITI 1s, 5s, and 10s), and dramatically faster than in *rbp* mutants ($p<0.002$ at all intervals) (Figure 6C,D). These data further support the conclusion that the defect in recovery from synaptic depression in *rbp* cannot be solely attributed to a reduction in presynaptic Ca^{2+} influx.

Finally, because the slowing of vesicle replenishment following repetitive stimulation is so dramatic in *rbp* mutants, we reasoned that the effects on release might be also observable after single AP stimulation instead of a stimulus train. This would also allow us to correlate presynaptic Ca^{2+} influx to neurotransmitter release during single AP stimulation. We, therefore, applied two APs using an inter-stimulus interval at which there is very little short-term release modulation at the *Drosophila* NMJ (1s; Figure 7; Müller et al., 2011). Under these conditions, wild-type synapses showed very modest synaptic depression (93±3% of control; 3mM $[Ca^{2+}]_e$). We observe a trend toward more pronounced synaptic depression in *rbp* mutants (82±6% of control; $p=0.07$ compared to wild type), even though the first EPSC in *rbp* is significantly smaller than in wild type ($p<0.001$; Figure 7A, left), which normally would be expected to diminish synaptic depression. Next, we normalized release between the two genotypes by testing *rbp* mutants at 15mM $[Ca^{2+}]_e$ and compared these data to wild type at 3mM $[Ca^{2+}]_e$. Under these conditions, there was no significant difference in initial EPSC amplitude between wild-type and *rbp* (Figure 7B, left; $p=0.21$), but paired-pulse depression was significantly enhanced in *rbp* (57±6% of control; Figure 7B, right; $p<0.001$). We then demonstrate that there is no significant difference in the paired-pulse ratio of presynaptic Ca^{2+} transient amplitudes between wild type (97±3% of control) and *rbp* (103±2% of control; Figure 7C; $p=0.37$), suggesting that enhanced paired-pulse depression in *rbp* is a not a secondary consequence of a defect in Ca^{2+} influx. Thus, our data imply that *rbp* is necessary for the replenishment of release-ready vesicles, independent of any decrease in presynaptic Ca^{2+} influx. Furthermore, the deficit in vesicle recovery is correlated with a profound change in the dynamics of release during repetitive stimulation (Fig 4, see also below).

Induction of Homeostatic Signaling Slows the Rate of Vesicle Recovery in *rbp*

We next asked whether the rates of vesicle recovery following a stimulus train are altered following the induction of homeostatic plasticity (Figure 5E, F). First, we analyzed wild type with and without PhTX at 3mM $[Ca^{2+}]_e$ and find that there is no change in vesicle replenishment rates between these two conditions (Figure 5E; $p\geq0.49$ for τ_{fast} and τ_{slow}). Next, we examined *rbp* mutants with and without PhTX at 15mM $[Ca^{2+}]_e$, again normalizing for diminished release-ready vesicle number in *rbp* compared to wild type. Remarkably, while the fast time constant was unaltered (Figure 5F; $p=0.48$), the slow time constant of vesicle recovery was slowed 3-fold compared to baseline recovery of *rbp* mutants (Figure 5F; $p=0.037$). The slow time constant in *rbp* (+PhTX) was ~ 60s, nearly ten-fold slower than that observed in wild type (+ PhTX) at 3mM $[Ca^{2+}]_e$. Remarkably, this pronounced homeostasis-dependent slowing of vesicle recovery was not seen when probing the recovery of the cumulative EPSC using a stimulus train instead of single EPSCs to chart the rate of vesicle recovery (Figure 5F, $p\geq0.25$ for τ_{fast} and τ_{slow}). The major difference between these assays is that intra-terminal Ca^{2+} accumulates during a stimulus train.

Therefore, the homeostasis-dependent rate limiting stage of vesicle recovery observed in *rbp* mutants can be surpassed by elevated intra-terminal Ca^{2+} (see discussion). Since the homeostatic change in RRP size and vesicle release are blocked in *rbp*, the slowing cannot be caused by increased vesicle usage. Rather, in the absence of RBP, a stage in the recovery of high release probability vesicles becomes sensitive to the induction of homeostatic signaling. Finally, an additional control was performed. We measured the rates of vesicle recovery in wild type in the presence of PhTX at 15mM $[Ca^{2+}]_e$ (Figure 5B, C). There was no change in the fast time constant of recovery upon PhTX application (not shown; p=0.42 for 1st EPSC), and a trend towards a PhTX-dependent slowing of the slow time constant, changing by approximately 3s (not shown; p=0.08). This change is much less pronounced than that observed in *rbp*, which slows by 34s, but highlights the possibility that the expansion of the RRP at a wild-type synapse at very high extracellular Ca^{2+} may also reveal a stage of vesicle recovery that is sensitive to the induction of homeostatic plasticity. As stated earlier, the fact that the RRP can be doubled at super-physiological Ca^{2+} concentrations, where the Ca^{2+}-dependence of release is saturated, suggests that additional post-translational changes in the release mechanism are required to double the size of the RRP. Whatever these changes are – they require RBP and appear to affect the rate at which high-release probability vesicles are recovered following synaptic depression.

Genetic interaction between *rbp* and *rim* during baseline synaptic transmission but not during homeostatic plasticity

RBP biochemically binds to RIM and we recently provided evidence that RIM is required for normal baseline synaptic transmission as well as homeostatic potentiation of presynaptic release (Müller et al., 2012). Therefore, we tested whether *rbp* and *rim* show a genetic interaction during baseline synaptic transmission and homeostatic plasticity. First, we tested baseline transmission, demonstrating that removal of one copy of either *rbp* or *rim* does not alter mEPSP, EPSP, and quantal content measurements compared to wild type ('− PhTX', 0.4mM $[Ca^{2+}]_e$; Figure 8A, all $p \geq 0.24$). However, when we examine *rbp*/+, *rim*/+ double heterozygous animals we find that EPSP amplitudes and quantal content are severely decreased with respect to wild type and either heterozygous single mutant alone (Figure 8A, purple data; all $p < 0.001$). This result indicates that RIM and RBP act upon the same processes to control baseline synaptic transmission, consistent with their known biochemical interaction and similar effects on the size of the RRP and Ca^{2+} influx under baseline conditions at the *Drosophila* NMJ.

As a control, we also tested a double heterozygous interaction of *rbp*/+ and Bruchpilot (*brp*/+). It was previously demonstrated that RBP localization to the active zone depends upon the presence of Brp, indicating a functional interaction (Liu et al., 2011). Here we demonstrate that EPSP amplitudes in double heterozygous animals harboring *brp*/+ and *rbp*/+ are nearly wild type (Figure 8A, green data, middle), with only a slight deficit in quantal content (Figure 8A, bottom). These data highlight the specificity of the defect observed in the *rbp*/+, *rim*/+ double heterozygous animals since the severity of this genetic interaction cannot be phenocopied by simply removing another active zone component (Brp), particularly one that is known to localize RBP protein to the active zone. Also, we note that the readily-releasable vesicle pool size is reduced in both*rbp* and *rim* mutants

(Figure 3, and Müller et al., 2012), but not in *brp* mutants (Hallermann et al., 2010c). Therefore, we speculate that the severe decrease in baseline transmission seen in double-heterozygous *rbp/+*, *rim/+* animals is due to a combined effect of these genes acting upon Ca^{2+} influx and the RRP.

We next probed homeostatic compensation in heterozygous *rbp/+* mutants at different $[Ca^{2+}]_e$ (Figure 8B). Wild-type EPSP amplitudes were similar in the absence and presence of PhTX at all $[Ca^{2+}]_e$ (all $p>0.17$), indicating normal homeostatic plasticity. By contrast, PhTX application significantly reduced EPSP amplitudes in *rbp/+* at the two lowest $[Ca^{2+}]_e$ as compared to baseline (Figure 8B, all $p<0.001$), while there was no significant difference at the highest $[Ca^{2+}]_e$ tested (1mM; Figure 8B, all $p>0.58$). Thus, homeostatic plasticity is normal in *rbp/+* at elevated $[Ca^{2+}]_e$, but becomes increasingly impaired as $[Ca^{2+}]_e$ is lowered, indicating that homeostatic plasticity is less robust to changes in extracellular Ca^{2+} after removal of one *rbp* copy.

The observation that homeostatic potentiation is normal in *rbp/+* mutants at elevated $[Ca^{2+}]_e$ (Figure 8B) allowed us to investigate homeostatic plasticity in double heterozygous *rbp/+*, *rim/+* mutants (Figure 8C). We find that baseline EPSP amplitudes and quantal content are significantly smaller in double heterozygous *rbp/+*, *rim/+* mutants compared to wild type ($p=0.015$). PhTX application significantly reduced mEPSP amplitudes ($p<0.001$) and potentiated quantal content in all genotypes ($p<0.001$), demonstrating that homeostatic plasticity proceeds normally in double heterozygous *rbp/+*, *rim/+* mutants. Thus, while *rbp/+* and *rim/+* fail to complement each other for baseline neurotransmitter release, they do complement each other for homeostatic plasticity, suggesting that each might bring a unique activity to the execution of homeostatic plasticity, an idea that is consistent with the differential effects of the homozygous *rim* and *rbp* mutants on the homeostatic regulation of presynaptic Ca^{2+} influx, and the rate of vesicle recovery.

DISCUSSION

RBP Stabilizes a High-Release Probability Vesicle Pool

RBP specifically localizes to a domain that surrounds the presynaptic CaV2.1 Ca^{2+} channel (Liu et al., 2011). Our data are consistent with previous analysis of baseline transmission in *rbp* mutants where it was shown that loss of RBP impairs the abundance and organization of Ca^{2+} channels at the active zone, causes a 30% drop in the amplitude of spatially averaged presynaptic Ca^{2+} transients and causes a striking >90% decrease in neurotransmitter release at physiological Ca^{2+} (Liu et al., 2011). Even though there is a supralinear relationship between Ca^{2+} influx and release, it is striking that release is nearly abolished in *rbp* while Ca^{2+} influx is decreased by only one third.

Here we present several lines of evidence that the defect in release observed in *rbp* mutants is due to the combined influence of 1) looser coupling of vesicles to the sites of presynaptic Ca^{2+} entry, and 2) impaired access to the RRP of synaptic vesicles. First, we confirm that there is only a modest, 28% decrease in presynaptic Ca^{2+} influx in *rbp* compared to wild type (Figure 2). Remarkably, this difference is diminished or eliminated as external Ca^{2+} is elevated beyond physiological levels (Figure 6A, 6B, 7C), whereas release remains strongly

impaired (Figure 1). The absence of an apparent difference in Ca2+ influx between wild type and rbp at elevated external Ca2+ levels could be due to effects of elevated external Ca2+ acting on presynaptic AP repolarization (Ford and Davis, 2014) or channel properties that eliminate the difference observed at lower Ca2+ concentrations. Regardless, when we analyze Ca2+ influx there is no difference comparing wild type and rbp at 3mM external Ca2+ and yet, under these precise recording conditions, there is a pronounced defect in presynaptic release. Thus, RBP must have an additional role in vesicle release. Second, we demonstrate that loss of *rbp* confers a very high EGTA sensitivity to synaptic transmission (Figure 3). This effect cannot be attributed to decreased presynaptic Ca^{2+} influx in the *rbp* mutant, because (i.) wild-type synapses display a very modest EGTA sensitivity when normalizing for presynaptic Ca^{2+} influx (Figure 3), and (ii.) a mutation that causes a similar defect in presynaptic Ca^{2+} influx (*rim*) induces a less pronounced EGTA sensitivity as compared to *rbp* (Müller et al., 2011). Since EGTA application to *rbp* mutant synapses reduces EPSC amplitudes by greater than 50%, the release-ready vesicles that support release in *rbp* mutants either have an 'intrinsically' low Ca^{2+} affinity that is independent of vesicle localization, or they are localized more distant from the Ca^{2+} channels compared to wild type. The latter possibility agrees with previous electron microscopy data showing a decrease in the number of vesicles located within 5nm of the presynaptic T-bar, which identifies the location of Ca^{2+} channels at this presynaptic active zone (Liu et al., 2011). These data are consistent with the conclusion that loss of RBP impairs either the formation or maintenance of a high-release probability vesicle pool that resides in close proximity to presynaptic Ca^{2+} channels where RBP has been shown to localize (Liu et al., 2011).

Analysis of recovery from synaptic depression reveals another activity of RBP that is essential for the formation and/or maintenance of a high-release probability pool of synaptic vesicles. We found that the slow kinetics of synaptic vesicle recovery following a depleting stimulus train is dramatically impaired (by ~400%, Figure 5). This effect far exceeds previously published studies characterizing a role for Munc-13, bassoon, or calmodulin in vesicle recovery after repetitive stimulation. The loss of any of these genes altered the slow phase of vesicle recovery by a maximum of 40% (Junge et al., 2004; Chen et al., 2013; Frank et al., 2010; Hallermann et al., 2010a; 2010b; Lipstein et al., 2013; Sakaba and Neher, 2001). Truncation of the C-terminal end of the presynaptic protein Bruchpilot specifically impairs the fast recovery phase (Hallermann et al., 2010a), while further truncation of the C-terminus of Bruchpilot (brp5.45 and brp 1.3; (Fouquet et al., 2009) affects both the slow and the fast recovery phase (Hallermann et al., 2010a). By comparison, the absence of RBP predominantly decelerates the slow recovery phase, and therefore likely plays a major role in stabilizing a high release-probability vesicle pool, an idea that is consistent with the other *rbp* phenotypes we report. By controlling the size and stability of the high-release probability vesicle pool, RBP would also effectively couple a change in Ca^{2+} influx to modulation of the RRP, both of which are required for the expression of homeostatic synaptic plasticity (see next section).

RBP and the homeostatic modulation of the RRP

The homeostatic potentiation of presynaptic neurotransmitter release requires an increase in the number of release-ready vesicles based upon either cumulative EPSC amplitude analysis

during brief, high-frequency stimulus trains, or variance-mean EPSC-amplitude analysis following single AP stimulation at low frequency (Müller et al., 2012; Weyhersmüller et al., 2011). At mammalian central synapses, RRP size correlates with extracellular Ca^{2+} concentration (Schneggenburger et al., 1999; Thanawala and Regehr, 2013). This raises the possibility that the homeostatic modulation of the RRP is simply a consequence of enhanced presynaptic Ca^{2+} influx. Our data demonstrate that this cannot be the case. First, the relationship between extracellular Ca^{2+} and RRP size is sublinear and quite shallow at high extracellular Ca^{2+} concentrations (Figure 3). During synaptic homeostasis, we observe a ~20-30% increase in presynaptic Ca^{2+} influx, which would not seem to be sufficient to achieve a doubling of the RRP based on the relationship between extracellular Ca^{2+} and RRP size (Figure 3D). Furthermore, we previously demonstrated that RIM is necessary for the homeostatic potentiation of RRP size, while not perturbing the homeostatic modulation of presynaptic Ca^{2+} influx (Müller et al., 2012), thereby providing a molecular separation between these two processes.

It is worth noting that baseline RRP size, estimated at physiological Ca^{2+}, is smaller in both *rbp* and *rim* mutants. As such, it is possible that loss of RIM or RBP could simply lead to a decrease in RRP size and thereby prevent homeostatic plasticity. However, we present data that argue against this possibility for *rbp* mutants. The absolute RRP size is equivalent when comparing wild type and *rbp* mutants at super-physiological extracellular Ca^{2+} (15mM), while the homeostatic modulation of RRP size is completely blocked (Figure 3, 4). It appears, therefore, that the total number of release-ready vesicles is not affected. Rather, access to the pool is impaired in *rbp.* Remarkably, RRP size is not nearing saturation when recording at 15mM extracellular Ca^{2+} because we are able to observe a homeostatic doubling of RRP size under these condition at wild-type terminals (Figure 4). Based on these data, we hypothesize that RBP recruits a biochemical activity during synaptic homeostasis through one of its protein interaction domains to expand the size of the RRP.

Loss of RBP reveals a rate limiting stage in vesicle resupply that is sensitive to presynaptic homeostasis

In wild type, when we record at super-physiological extracellular Ca^{2+} (3mM), the induction of presynaptic homeostasis has no effect on the kinetics of synaptic vesicle replenishment following a stimulus train (Figure 5). Thus, recovery rates are insensitive to the absolute number of vesicles that are released during a depleting stimulus train, since release is doubled following the induction of synaptic homeostasis at all Ca^{2+} concentrations tested (Figure 1E). However, in *rbp* mutants, the induction of homeostatic plasticity decelerates the slow phase of vesicle recovery by ~300%. This is remarkable because the slow rate of recovery is already decelerated at baseline in *rbp* mutants by ~400% compared to wild type (Figure 5). The combined effect is that vesicles that take ~6s to recover in wild type now take nearly 60s to recover in *rbp* following the induction of homeostatic plasticity. The additional deceleration observed in *rbp* following the induction of homeostatic plasticity is not a secondary consequence of releasing additional vesicles during the depleting stimulus train, because this does not happen in the *rbp* mutant. We conclude that the absence of RBP has revealed a step in the process of vesicle replenishment that becomes rate limiting following the induction of presynaptic homeostasis. It is possible that this step could be

normally acted upon by the homeostatic signaling system to ensure that the homeostatically enhanced state of release can be sustained during the repetitive stimulation that is characteristic of normal neuromuscular activity. Indeed, this RBP-dependent step could be related to the observation that the size of the RRP actually decreases instead of increasing following the induction of presynaptic homeostasis (Figure 4B).

Several additional observations argue that the homeostasis-dependent deficit in vesicle recovery is not simply a secondary consequence of an impaired active zone. First, the homeostasis-dependent deceleration of replenishment kinetics is largely confined to the high-release probability population of vesicles, because the fast component of recovery is essentially unaltered (Figure 5). Second, the slow rate of recovery is unaltered if one probes recovery of the vesicle pool using stimulus trains. During stimulus trains, as opposed to single AP stimulation, Ca^{2+} levels rise substantially. We conclude that the rate limiting stage of vesicle recovery is sensitive to the concentration of intracellular Ca^{2+}, consistent with the known role of Ca^{2+} in accelerating vesicle replenishment (Neher and Sakaba, 2008). This argues that the process of vesicle recovery is not simply broken following the loss of RBP. Finally, previous ultrastructural examination of the active zone in *rbp* showed no evidence of accumulated membrane material that might indicate a ‘traffic jam’ at the active zone.

It is straightforward to suggest that the loss of *rbp* prevents the capture or stabilization of vesicles at the active zone, thereby dramatically decelerating the rate of vesicle replenishment to this pool under baseline conditions. If the number of vesicles being replenished remains unaltered in *rbp* mutants following the induction of synaptic homeostasis, then what accounts for the additional deceleration? It seems that the induction of homeostatic plasticity induces an additional presynaptic process that becomes rate limiting in the absence of RBP. In this study, we demonstrate that the RRP can be doubled, even in the presence of 15mM extracellular Ca^{2+}, suggesting a rather remarkable change in vesicle usage. It seems likely that this is achieved through the conversion of vesicles from the reserve pool to the RRP. One possibility is that this conversion process is still induced, but it becomes rate limiting in the absence of RBP. This would position RBP downstream in the cascade of events that lead to a functional doubling of the RRP, which is consistent with the localization of RBP at the Ca^{2+} channel. Finally, since loss of RIM has no effect on the rate of recovery yet also blocks the expansion of the RRP, the mechanism by which RIM acts on the RRP must be distinct. This possibility remains consistent with our genetic interaction experiments (Figure 8).

RBP and the modulation of presynaptic Ca^{2+} influx

In addition to being crucial for the homeostatic modulation of RRP size, we also provide evidence that RBP is required for the homeostatic enhancement of presynaptic Ca^{2+} influx (Figure 2). A RBP-mediated modulation of presynaptic Ca^{2+} influx is conceivable because RBP biochemically interacts with the C- terminus of the presynaptic voltage-gated Ca^{2+} channel (Hibino et al., 2002; Liu et al., 2011). Moreover, RBP has been recently shown to be required for normal Ca^{2+} channel density at active zones and normal Ca^{2+} influx levels (Liu et al., 2011). Recent data indicate that low-voltage modulation of the presynaptic membrane via insertion of DEG/ENaC sodium leak channels may be a mechanism for

altering presynaptic Ca^{2+} influx during presynaptic homeostasis (Younger et al., 2012). In this context, RBP may be required for the responsivity of the presynaptic CaV2.1 Ca^{2+} channels to membrane voltage changes.

Biochemical data provide insight into the unique activities of RIM and RBP. *Drosophila* RBP specifically interacts with the PxxP motifs of both RIM and the presynaptic voltage-gated Ca^{2+} channel through its third SH3 domain (Liu et al., 2011) (Figure 1A, bottom). It is therefore likely that RBP is either bound to RIM or to the Ca^{2+} channel, and that RBP's role in RRP size regulation and Ca^{2+} influx modulation might be biochemically separable. RIM interacts with a specific sequence at the very end of the C-terminus of the Ca^{2+} channel through its PDZ domain. Thus, RIM and RBP bind to different domains of the Ca^{2+} channel's C-terminus, which might explain the different roles of RBP and RIM in the homeostatic regulation of Ca^{2+} influx.

EXPERIMENTAL PROCEDURES

Fly Stocks and Genetics

Drosophila stocks were maintained at 22 – 25 °C on normal food. rbp^{STOP1}, $rbp^{S2.01}$ (Liu et al., 2011), *rim103* (Müller et al., 2012), and brp^{69} mutant flies (Kittel et al., 2006) were obtained from the Sigrist lab. The w^{1118} strain was used as a wild-type control. rbp^{STOP1}/$rbp^{S2.01}$ 2nd instar larvae were separated from heterozygous larvae, and raised in isolation before recordings.

Electrophysiology

Sharp-electrode recordings were made from muscle 6 in abdominal segments 2 and 3 of third instar larvae using an Axopatch 200B, or a Multiclamp 700B amplifier (Axon Instruments), as previously described (Davis and Goodman, 1998). The apparent size of the readily-releasable vesicle pool (RRP) was probed by the method of cumulative EPSC amplitudes (Schneggenburger et al., 1999), which was recently applied to the *Drosophila* NMJ (Hallermann et al., 2010c; Miśkiewicz et al., 2011; Müller et al., 2012; Weyhersmüller et al., 2011) (see also supplemental methods).

Ca^{2+} Imaging

Ca^{2+} imaging experiments were done as described in Müller and Davis (2012; see also supplemental methods). Third instar larvae were dissected and incubated in ice cold, Ca^{2+}-free HL3 containing 5 mM Oregon-Green 488 BAPTA-1 (OGB-1; hexapotassium salt, Invitrogen) and 1 mM Alexa 568 (Invitrogen). After incubation for 10 minutes, the preparation was washed with ice cold HL3 for 10 – 15 minutes. This lead to an intraterminal OGB-1 concentration of approximately 50 μM (Müller and Davis, 2012). Single action-potential evoked spatially-averaged Ca^{2+} transients were measured in type-1b boutons synapsing onto muscle 6/7 of abdominal segments A2/A3 at an extracellular $[Ca^{2+}]$ of 1 mM using a confocal laser-scanning system (Ultima, Prairie Technologies) at room temperature. Fluorescence changes were quantified as $\Delta F/F = (F(t)- F_{baseline})/(F_{baseline}-F_{background})$, where F(t) is the fluorescence in a region of interest (ROI) containing a bouton at any given time, $F_{baseline}$ is the mean fluorescence from a 300-ms period preceding the stimulus, and

$F_{background}$ is the background fluorescence from an adjacent ROI without any indicator-containing cellular structures.

Data Analysis

Electrophysiology data was acquired with Clampex (Axon Instruments), and imaging data was recorded with Prairie View (Prairie Technologies). Data were analyzed with custom-written routines using Igor Pro 6.2.2. (Wavemetrics), and mEPSPs were analyzed with Mini Analysis 6.0.3. (Synaptosoft). Statistical significance was assessed with a Student's t-test, and all error bars are SEM.

Supplementary Material

Refer to Web version on PubMed Central for supplementary material.

REFERENCES

Burrone J, O'Byrne M, Murthy VN. Multiple forms of synaptic plasticity triggered by selective suppression of activity in individual neurons. Nature. 2002; 420:414–418. [PubMed: 12459783]

Chen Z, Cooper B, Kalla S, Varoqueaux F, Young SM. The Munc13 proteins differentially regulate readily releasable pool dynamics and Ca^{2+}-dependent recovery at a central synapse. Journal of Neuroscience. 2013; 33:8336–8351. [PubMed: 23658173]

Davis GW, Goodman CS. Synapse-specific control of synaptic efficacy at the terminals of a single neuron. Nature. 1998; 392:82–86. [PubMed: 9510251]

Davis GW. Homeostatic control of neural activity: from phenomenology to molecular design. Annu. Rev. Neurosci. 2006; 29:307–323. [PubMed: 16776588]

Ford KJ, Davis GW. Archaerhodopsin Voltage Imaging: Synaptic Calcium and BK Channels Stabilize Action Potential Repolarization at the Drosophila Neuromuscular Junction. Journal of Neuroscience. 2014; 34:14517–14525. [PubMed: 25355206]

Fouquet W, Owald D, Wichmann C, Mertel S, Depner H, Dyba M, Hallermann S, Kittel RJ, Eimer S, Sigrist SJ. Maturation of active zone assembly by Drosophila Bruchpilot. The Journal of Cell Biology. 2009; 186:129–145. [PubMed: 19596851]

Frank CA, Kennedy MJ, Goold CP, Marek KW, Davis GW. Mechanisms underlying the rapid induction and sustained expression of synaptic homeostasis. Neuron. 2006; 52:663–677. [PubMed: 17114050]

Frank CA, Pielage J, Davis GW. A Presynaptic Homeostatic Signaling System Composed of the Eph Receptor, Ephexin, Cdc42, and CaV2.1 Calcium Channels. Neuron. 2009; 61:556–569. [PubMed: 19249276]

Frank T, Rutherford MA, Strenzke N, Neef A, Pangršič T, Khimich D, Fejtova A, Fetjova A, Gundelfinger ED, Liberman MC, et al. Bassoon and the synaptic ribbon organize Ca^{2+} channels and vesicles to add release sites and promote refilling. Neuron. 2010; 68:724–738. [PubMed: 21092861]

Hallermann S, Kittel RJ, Wichmann C, Weyhersmüller A, Fouquet W, Mertel S, Owald D, Eimer S, Depner H, Schwarzel M, et al. Naked Dense Bodies Provoke Depression. Journal of Neuroscience. 2010a; 30:14340–14345. [PubMed: 20980589]

Hallermann S, Silver RA. Sustaining rapid vesicular release at active zones: potential roles for vesicle tethering. Trends Neurosci. 2013; 36:185–194. [PubMed: 23164531]

Hallermann S, Fejtova A, Schmidt H, Weyhersmüller A, Silver RA, Gundelfinger ED, Eilers J. Bassoon speeds vesicle reloading at a central excitatory synapse. Neuron. 2010b; 68:710–723. [PubMed: 21092860]

Hallermann S, Heckmann M, Kittel RJ. Mechanisms of short-term plasticity at neuromuscular active zones of Drosophila. HFSP Journal. 2010c; 4:72–84. [PubMed: 20811513]

Hibino H, Pironkova R, Onwumere O, Vologodskaia M, Hudspeth AJ, Lesage F. RIM binding proteins (RBPs) couple Rab3-interacting molecules (RIMs) to voltage-gated Ca^{2+} channels. Neuron. 2002; 34:411–423. [PubMed: 11988172]

Junge HJ, Rhee J-S, Jahn O, Varoqueaux F, Spiess J, Waxham MN, Rosenmund C, Brose N. Calmodulin and Munc13 Form a Ca^{2+} Sensor/Effector Complex that Controls Short-Term Synaptic Plasticity. Cell. 2004; 118:389–401. [PubMed: 15294163]

Kim SH, Ryan TA. CDK5 Serves as a Major Control Point in Neurotransmitter Release. Neuron. 2010; 67:797–809. [PubMed: 20826311]

Lipstein N, Sakaba T, Cooper BH, Lin K-H, Strenzke N, Ashery U, Rhee J-S, Taschenberger H, Neher E, Brose N. Dynamic control of synaptic vesicle replenishment and short-term plasticity by Ca($^{2+}$)-calmodulin-Munc13-1 signaling. Neuron. 2013; 79:82–96. [PubMed: 23770256]

Liu KSY, Siebert M, Mertel S, Knoche E, Wegener S, Wichmann C, Matkovic T, Muhammad K, Depner H, Mettke C, et al. RIM-binding protein, a central part of the active zone, is essential for neurotransmitter release. Science. 2011; 334:1565–1569. [PubMed: 22174254]

Miśkiewicz K, Jose LE, Bento-Abreu A, Fislage M, Taes I, Kasprowicz J, Swerts J, Sigrist S, Versées W, Robberecht W, et al. ELP3 Controls Active Zone Morphology by Acetylating the ELKS Family Member Bruchpilot. Neuron. 2011; 72:776–788. [PubMed: 22153374]

Müller M, Davis GW. Transsynaptic control of presynaptic Ca^{2+} influx achieves homeostatic potentiation of neurotransmitter release. Curr. Biol. 2012; 22:1102–1108. [PubMed: 22633807]

Müller M, Liu KSY, Sigrist SJ, Davis GW. RIM controls homeostatic plasticity through modulation of the readily-releasable vesicle pool. Journal of Neuroscience. 2012; 32:16574–16585. [PubMed: 23175813]

Müller M, Pym ECG, Tong A, Davis GW. Rab3-GAP Controls the Progression of Synaptic Homeostasis at a Late Stage of Vesicle Release. Neuron. 2011; 69:749–762. [PubMed: 21338884]

Plomp JJ, van Kempen GT, Molenaar PC. Adaptation of quantal content to decreased postsynaptic sensitivity at single endplates in alpha-bungarotoxin-treated rats. J Physiol (Lond). 1992; 458:487–499. [PubMed: 1302275]

Sakaba T, Neher E. Calmodulin mediates rapid recruitment of fast-releasing synaptic vesicles at a calyx-type synapse. Neuron. 2001; 32:1119–1131. [PubMed: 11754842]

Schneggenburger R, Meyer AC, Neher E. Released fraction and total size of a pool of immediately available transmitter quanta at a calyx synapse. Neuron. 1999; 23:399–409. [PubMed: 10399944]

Smith PD, Liesegang GW, Berger RL, Czerlinski G, Podolsky RJ. A stopped-flow investigation of Ca^{2+} ion binding by ethylene glycol bis(beta-aminoethyl ether)-N,N'-tetraacetic acid. Anal. Biochem. 1984; 143:188–195. [PubMed: 6442108]

Thanawala MS, Regehr WG. Presynaptic Ca^{2+} influx controls neurotransmitter release in part by regulating the effective size of the readily releasable pool. Journal of Neuroscience. 2013; 33:4625–4633. [PubMed: 23486937]

Thiagarajan TC, Lindskog M, Tsien RW. Adaptation to synaptic inactivity in hippocampal neurons. Neuron. 2005; 47:725–737. [PubMed: 16129401]

Weyhersmüller A, Hallermann S, Wagner N, Eilers J. Rapid Active Zone Remodeling during Synaptic Plasticity. Journal of Neuroscience. 2011; 31:6041–6052. [PubMed: 21508229]

Wu L-G, Borst JG. The reduced release probability of releasable vesicles during recovery from short-term synaptic depression. Neuron. 1999; 23:821–832. [PubMed: 10482247]

Younger MA, Müller M, Tong A, Pym EC, Davis GW. A Presynaptic ENaC Channel Drives Homeostatic Plasticity. Neuron. 2013; 79:1183–1196. [PubMed: 23973209]

Zhao C, Dreosti E, Lagnado L. Homeostatic Synaptic Plasticity through Changes in Presynaptic Calcium Influx. Journal of Neuroscience. 2011; 31:7492–7496. [PubMed: 21593333]

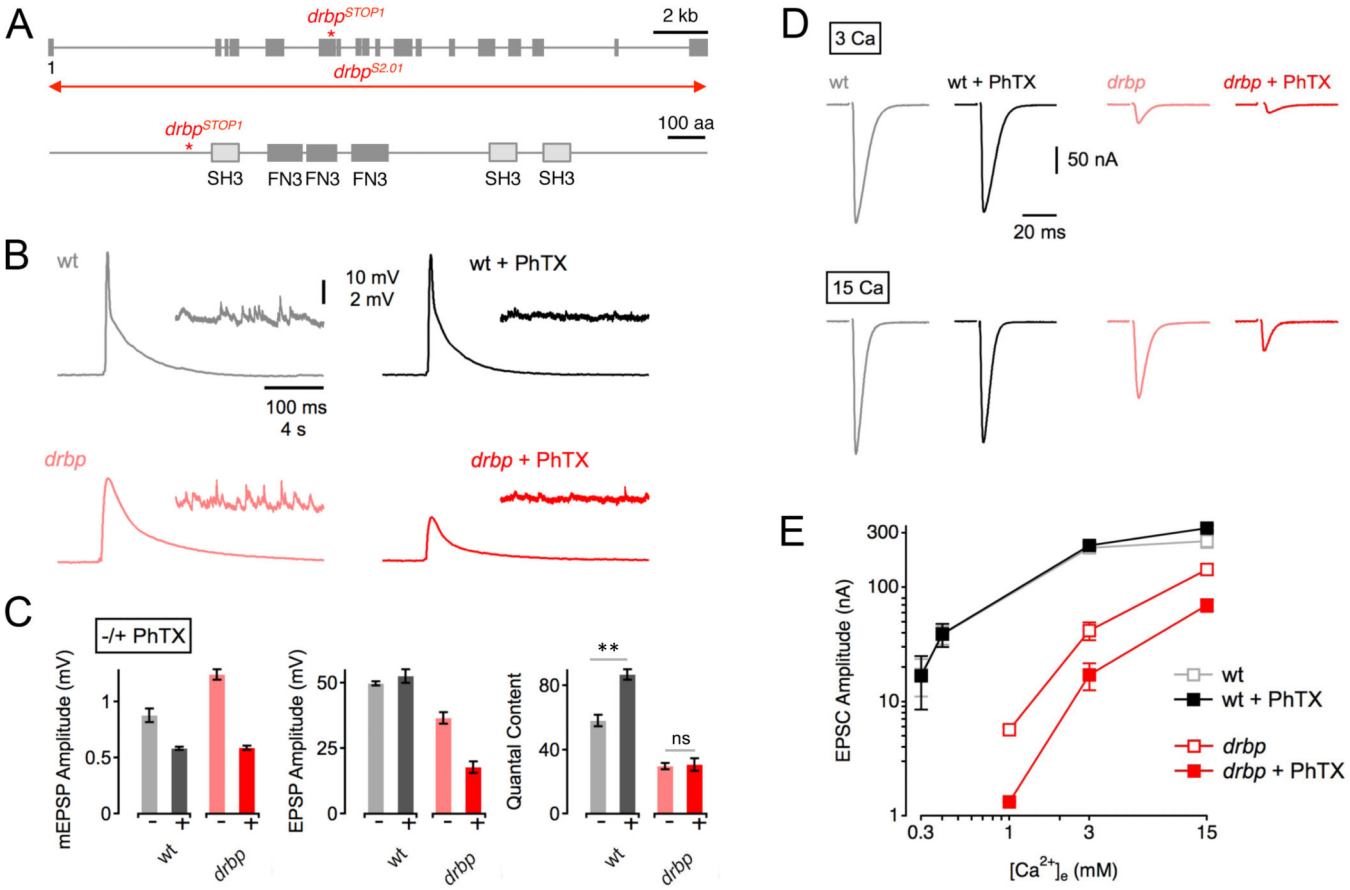

Figure 1. RIM-Binding Protein Is Required for Homeostatic Synaptic Plasticity

(A) Top: Schematic of the *drbp* locus indicating the approximate location of the $drbp^{STOP1}$ mutation. The 19 coding exons are represented by gray boxes ('1' denotes the first exon), and the red line refers the approximate location of the $drbp^{S2.01}$ deletion. Bottom: Schematic of RBP protein structure. Boxes denote the locations of the Src homology 3 domains (SH3), and the fibronectin type 3 (FN3) domains.

(B) Representative traces of EPSPs and mEPSPs for wild type in the absence and presence of PhTX (gray and black data; respectively), and $drbp^{STOP1}$ placed over the deficiency $drbp^{S2.01}$ in the absence and presence of PhTX (‘*drbp*’; light red, and dark red data; respectively; 1.5mM $[Ca^{2+}]_e$).

(C) Average mEPSP amplitudes (left), EPSP amplitudes (middle), and quantal content (EPSP/mEPSP; right) of the indicated genotypes minus PhTX (light gray/red) and plus PhTX (black, dark red). w^{1118} (−PhTX): n=8; w^{1118} (+PhTX): n=7; *drbp* (−PhTX): n=16; *drbp* (+PhTX): n=17.

(D) Sample EPSCs of the indicated genotypes in the absence and presence of PhTX (‘−/+ PhTX’) at 3mM $[Ca^{2+}]_e$ (top row) and 15mM $[Ca^{2+}]_e$ (bottom row).

(E) Relationship between mean EPSC amplitude and extracellular Ca^{2+} concentration in wild type (control: light gray, n=4–7 per $[Ca^{2+}]_e$; PhTX: dark gray, n=4–7 per $[Ca^{2+}]_e$), and *drbp* (control: light red, n=8–12 per $[Ca^{2+}]_e$; PhTX: dark red, n=6–12 per $[Ca^{2+}]_e$). The wild-type data for the two lowest $[Ca^{2+}]_e$ were already published (Müller et al., 2012).

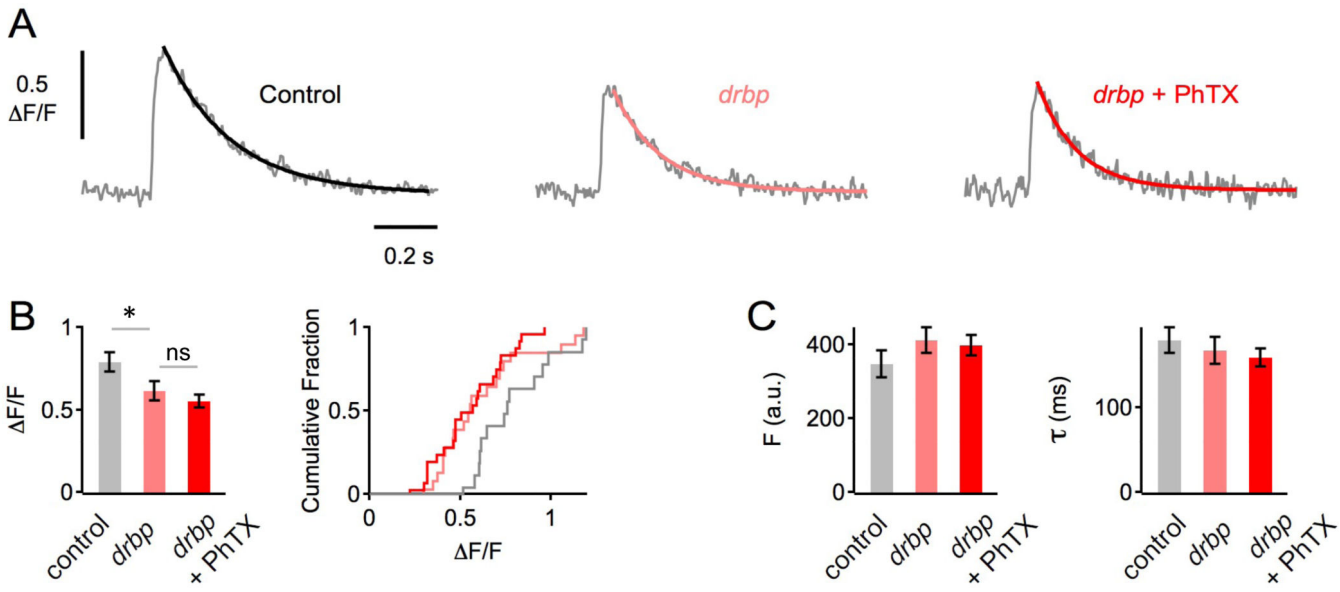

Figure 2. *rbp* Blocks the Homeostatic Enhancement of Presynaptic Ca^{2+} Influx

(A) Representative spatially-averaged Ca^{2+} transients of a wild-type control synapse and two *drbp* synapses in the absence (light red) and presence (dark red) of PhTX (average of 8 – 12 scans each; 1mM $[Ca^{2+}]_e$).

(B) Bar graph (left) and cumulative frequency plot (right) of average Ca^{2+}-transient peak amplitudes (ΔF/F) of control (ΔF/F=0.79±0.06; n=14 boutons; gray), *drbp* without PhTX (ΔF/F=0.61±0.06; n=20; light red), and *drbp* with PhTX (ΔF/F=0.55±0.04; n=24; dark red). Ca^{2+} transients in *drbp* mutants are significantly smaller than in control under baseline conditions (p=0.049), and there is no significant difference in peak amplitude between *drbp* in the absence and presence of PhTX (p=0.37).

(C) Average baseline fluorescence ('F') and decay time constant ('τ') of the indicated genotypes and conditions.

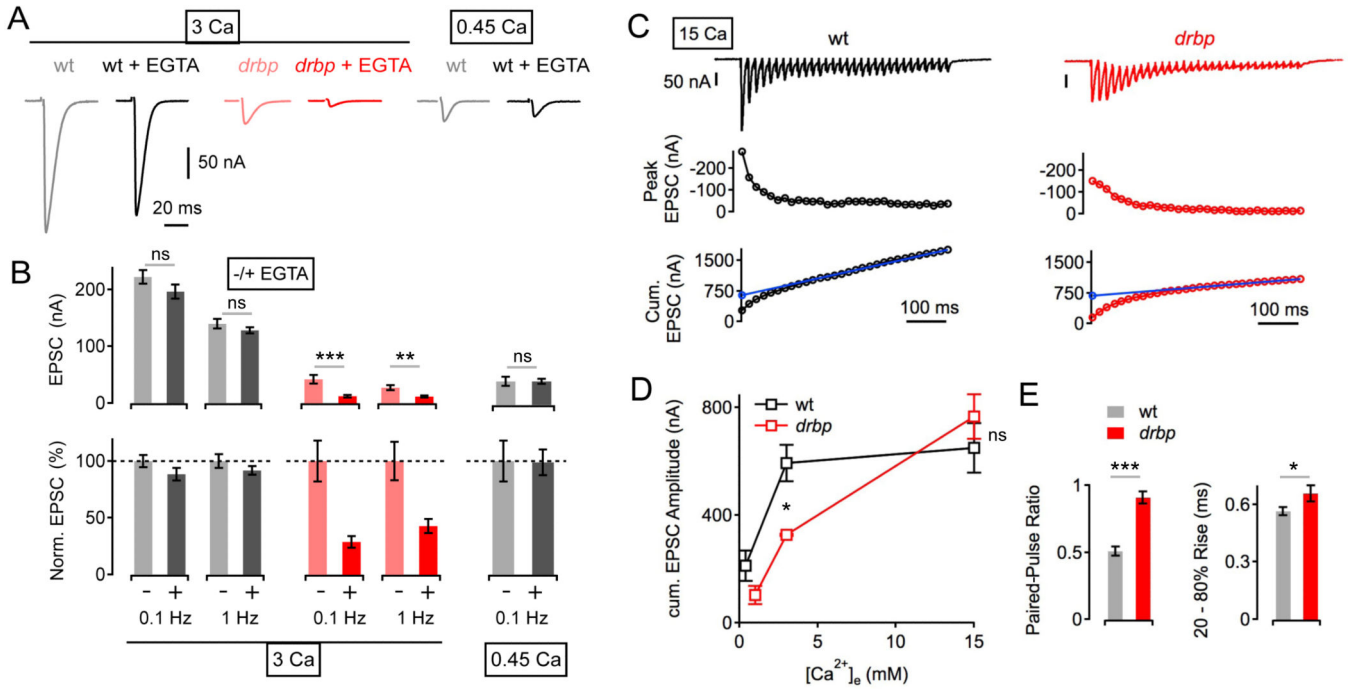

Figure 3. Increased EGTA-Sensitivity and Reduced Readily-Releasable Vesicle Pool Size after Loss of *rbp*

(A) Example EPSC traces of wild type and *drbp* mutants under control conditions, and after incubation in 25μM EGTA-AM for 10 minutes (stimulation frequency, 0.1 Hz) at 3mM $[Ca^{2+}]_e$ ('3 Ca', left), or 0.45mM $[Ca^{2+}]_e$ ('0.45 Ca', right).

(B) Average EPSC amplitudes (left) and normalized EPSC amplitudes (right) in the absence (−) and presence (+) of EGTA at the indicated stimulation frequencies and $[Ca^{2+}]_e$. 3 Ca: wt (−EGTA): n=7; wt (+EGTA): n=6; *drbp* (−EGTA): n=8; *drbp* (+EGTA): n=8; 0.45 Ca: wt (−EGTA): n=8; wt (+EGTA): n=10. Note the pronounced decrease in EPSC amplitude in *drbp* mutants upon EGTA treatment (p=0.001 and p=0.002 at 0.1Hz and 2Hz, respectively).

(C) EPSC trace (top), peak EPSC amplitudes (middle), and cumulative EPSC amplitudes ('cum. EPSC'; bottom) evoked by 60-Hz stimulation (30 stimuli) of a wild-type synapse (left) and a *drbp* synapse (right) at 15 mM $[Ca^{2+}]_e$. The line fit to the cumulative EPSC data that was back-extrapolated to time zero is shown in blue (see Experimental Procedures).

(D) Average cumulative EPSC amplitudes of wild type (black data; n=5–13 per $[Ca^{2+}]_e$) and *drbp* (red data; n=4–9 per $[Ca^{2+}]_e$) as a function of $[Ca^{2+}]_e$. Note the significant difference in cumulative EPSC amplitude between wild type and *drbp* at 3mM $[Ca^{2+}]_e$ (p=0.04), and the similarity in cumulative EPSC amplitude at the highest $[Ca^{2+}]_e$ tested (p=0.19).

(E) Average paired-pulse ratio (EPSC2/EPSC1, 60-Hz stimulation, left), and 20-80% EPSC rise time (right) at 15 mM $[Ca^{2+}]_e$ of wild type (n=6), and *drbp* mutants (n=9).

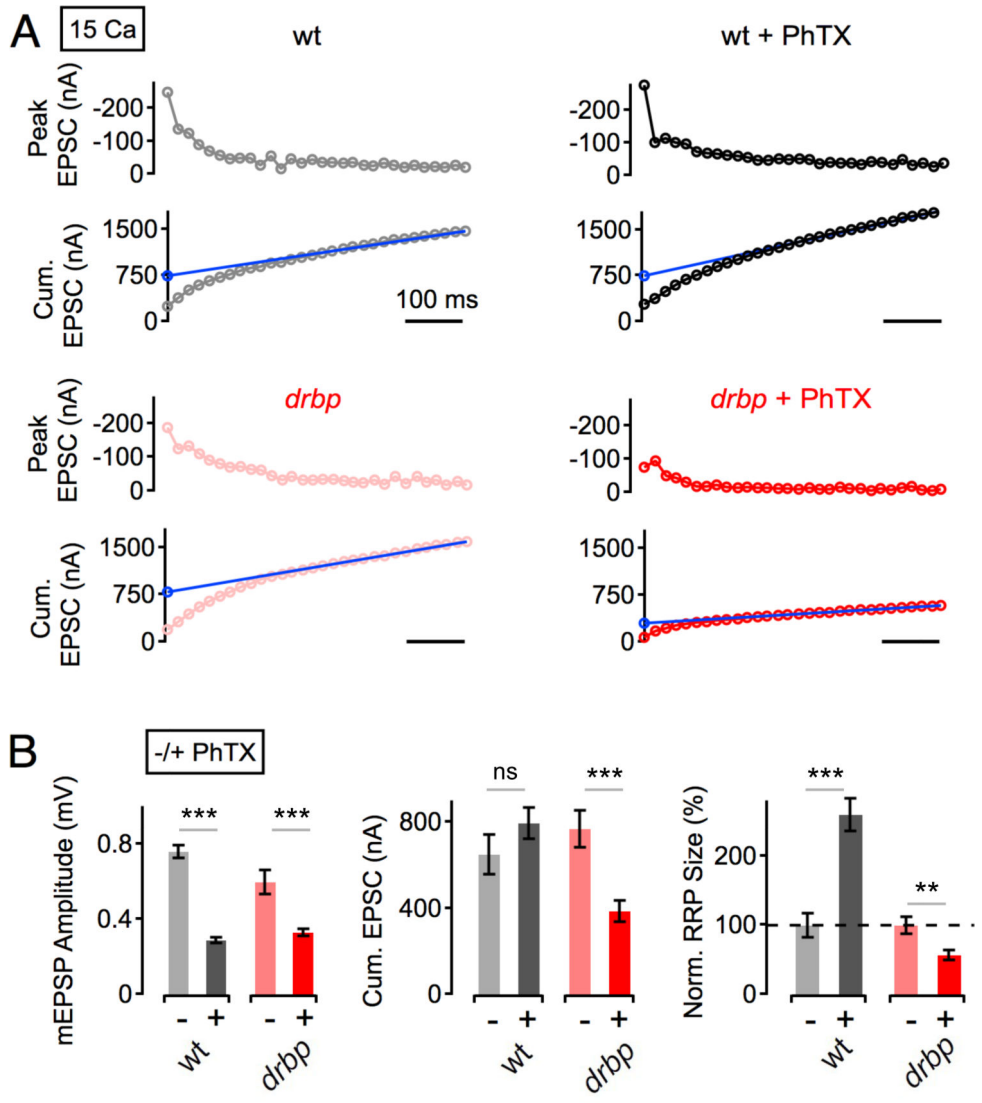

Figure 4. Homeostatic Modulation of Readily-Releasable Vesicle Pool Size is Absent in *rbp* Mutants

(A) Peak EPSC amplitudes (top), and cumulative EPSC amplitudes ('cum. EPSC'; bottom) during 60-Hz stimulation of representative synapses of the indicated genotypes in the absence (left) and presence (right) of PhTX at 15 mM $[Ca^{2+}]_e$.

(B) Average mEPSP amplitudes (left), cumulative EPSC amplitudes (middle), and normalized readily-releasable pool sizes ('RRP', right; see Experimental Procedures) of the indicated genotypes and conditions. wt (−PhTX): n=5; wt (+PhTX): n=7; *drbp* (−PhTX): n=9; *drbp* (+PhTX): n=12. PhTX application induces no significant change in cumulative EPSC amplitude in wild type (p=0.2), and a significant decrease in cumulative EPSC amplitude in *drbp* (p<0.001), indicating a block in the homeostatic increase in RRP size in *drbp*.

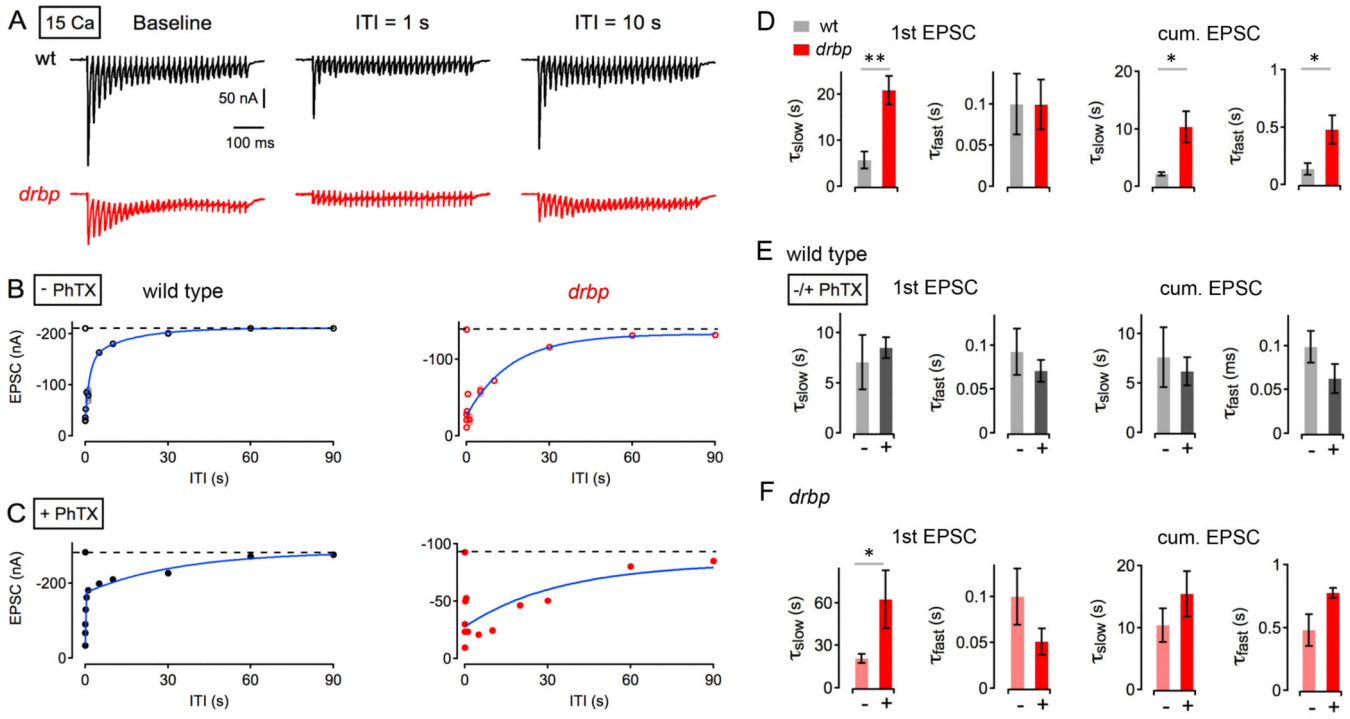

Figure 5. Slow Recovery From Synaptic Depression in *rbp*

(A) Sample EPSCs evoked by 60-Hz stimulation after a prolonged period of rest (no stimulation for at least 30s; 'baseline') and at inter-train intervals ('ITI') of 1s (middle) and 10s (right) of a wild type (top) and a *drbp* synapse (bottom) at 15 mM $[Ca^{2+}]_e$.

(B) Peak amplitudes of the first EPSC of the second 'test' train (top) and cumulative EPSC amplitudes (bottom) as a function of ITI of a wild-type (left) and a *rbp* mutant synapse (right) under baseline conditions ('− PhTX'). Average data and individual data for each synapse are shown in dark and light colors, respectively. Average data were fitted with a double-exponential function (blue).

(C) Representative EPSC recovery time courses of the indicated genotypes in the presence of PhTX ('+ PhTX').

(D) *1st EPSC*: Average slow time constants ('τ_{slow}'; left) and fast time constants ('τ_{fast}'; right) of exponential fits to the first EPSC amplitudes of the second train ('1st EPSC') of the indicated genotypes at 15 mM $[Ca^{2+}]_e$ and 3 mM $[Ca^{2+}]_e$. wt (15mM $[Ca^{2+}]_e$, n=4; 3mM $[Ca^{2+}]_e$, n=7), *drbp* (15mM $[Ca^{2+}]_e$, n=7) under baseline conditions. *cum. EPSC*: Average cumulative EPSC amplitudes of the same data set. We did not detect significant changes in the amplitudes of the slow and the fast exponential component for 1st EPSC and cumulative EPSC data between genotypes.

(E) Average recovery time constants of the 1st EPSC (left) and cum. EPSC in wild type in the absence and presence of PhTX ('−/+ PhTX') at 3mM $[Ca^{2+}]_e$ (n=7). There were no significant changes in recovery time constants in the absence and presence of PhTX (all $p \geq 0.29$).

(F) Average recovery time constants of the 1st EPSC (left) and cum. EPSC in *drbp* in the absence and presence of PhTX ('−/+ PhTX') at 15mM $[Ca^{2+}]_e$ (n=7). Note the significant slowing of τ_{slow} upon PhTX application (left; p=0.037).

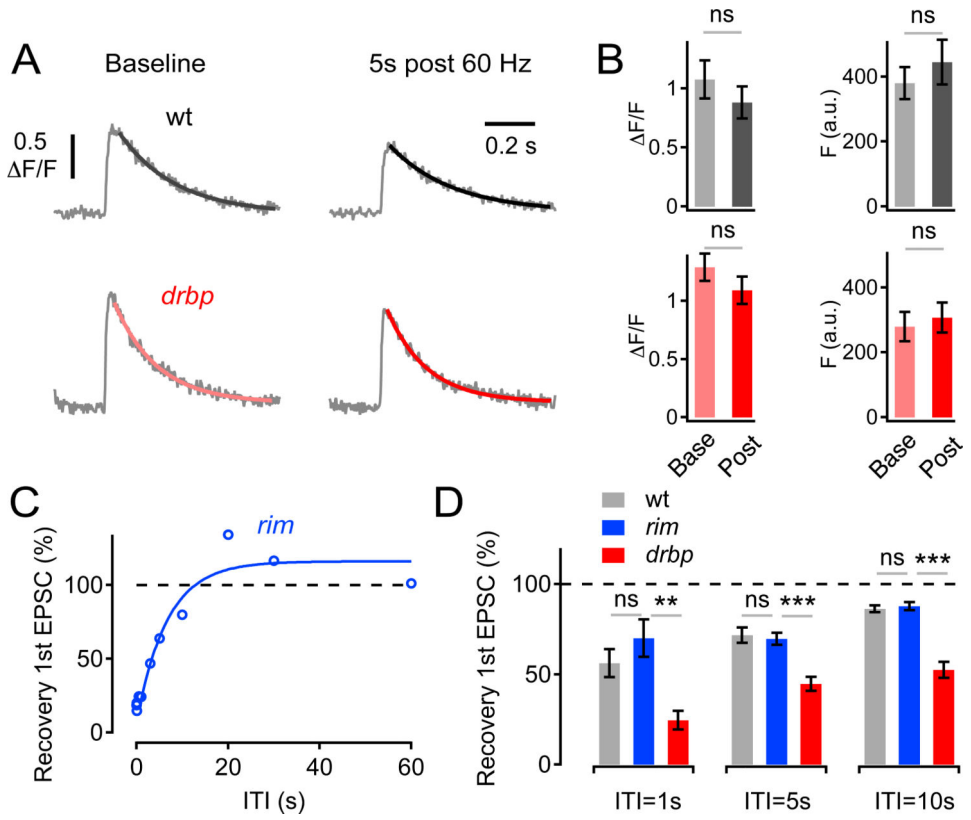

Figure 6. Unaltered Presynaptic Ca^{2+} Signaling During Recovery in *rbp*, and Normal Recovery From Synaptic Depression in *rim*

(A) Single AP-evoked spatially-averaged Ca^{2+} transients of a wild-type and a *drbp* synapse before ('baseline', left) and 5s after 60-Hz stimulations (30 stimuli, '5s post 60 Hz', right) (average of 4–9 scans each; 3mM $[Ca^{2+}]_e$).

(B) Average Ca^{2+}-transient peak amplitude (ΔF/F) and baseline fluorescence ('F') before ('Base') and after ('Post') 60-Hz stimulation of control (F (base) =380±55 a.u., F (post) =445±77 a.u., n=5, p=0.46; ΔF/F (base) =1.08±0.18, ΔF/F (post) =0.88±0.15, p=0.38, gray data), and *drbp* (F (base) =290±51 a.u., F (post) =320±52 a.u., n=10, p=0.66; ΔF/F (base) =1.29±0.12, ΔF/F (post) =1.09±0.12, p=0.25, red data). Note that there is no significant difference in the relative decrease in ΔF/F following 60-Hz stimulation between wild type (82±4% of control) and *drbp* (84±3% of control; p=0.58).

(C) Peak amplitudes of the first EPSC of 60-Hz 'test' trains normalized to the first EPSC of 60-Hz 'depleting' trains applied at various inter-train intervals of a *rim103* mutant synapse (30 stimuli per train). Data were fitted with a double-exponential function (blue).

(D) Average recovery of 1st EPSC amplitude following 60-Hz stimulation at the indicated ITIs of wild type (n=6), *rim103* (n=6), and *drbp* (n=6). Note that EPSC recovery from depression in *drbp* is significantly slower than in *rim* or wild type (p<0.002 at all intervals).

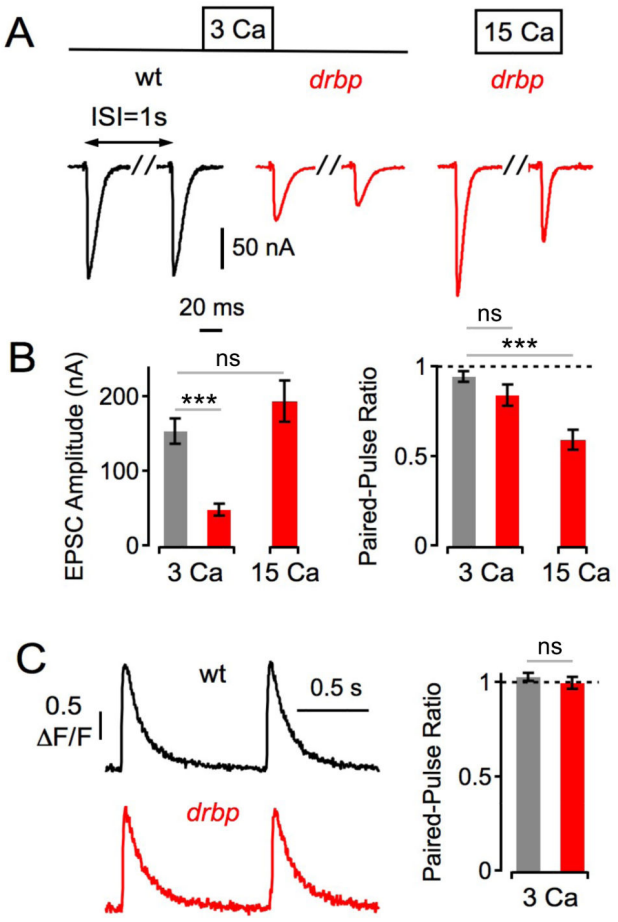

Figure 7. Slow Recovery From Synaptic Depression after Single-AP Stimulation in *rbp*

(A) Representative EPSCs in response to paired-pulse stimulation at an inter-stimulus interval (ISI) of 1s of the indicated genotypes and $[Ca^{2+}]_e$.

(B) Average first EPSC amplitudes (left) and paired-pulse ratio (EPSC2/EPSC1, right) of wt (3 Ca: n=8), *drbp* (3 Ca: n=8; 15 Ca: n=5). Note the similar first EPSC amplitudes (p=0.21), and the significant difference in paired-pulse ratio (p<0.001) between *drbp* at 15 Ca and wild type at 3 Ca.

(C) Left: Example spatially-averaged Ca^{2+} transients of wild type and a *drbp* induced by paired-pulse stimulation at an interval of 1s (average of 7–10 scans each; 3mM $[Ca^{2+}]_e$). Right: Average Ca^{2+}-transient amplitude paired-pulse ratio (ΔF/F2/(ΔF/F1)) of wild type (n=11) and a *drbp* (n=12). Note that we did not detect significant differences in baseline ΔF/F (wild type: 1.29 ± 0.11; *drbp*: 1.37 ± 0.0; p=0.52), and baseline fluorescence (p=0.99) at this $[Ca^{2+}]_e$ (see also Figure 6B).

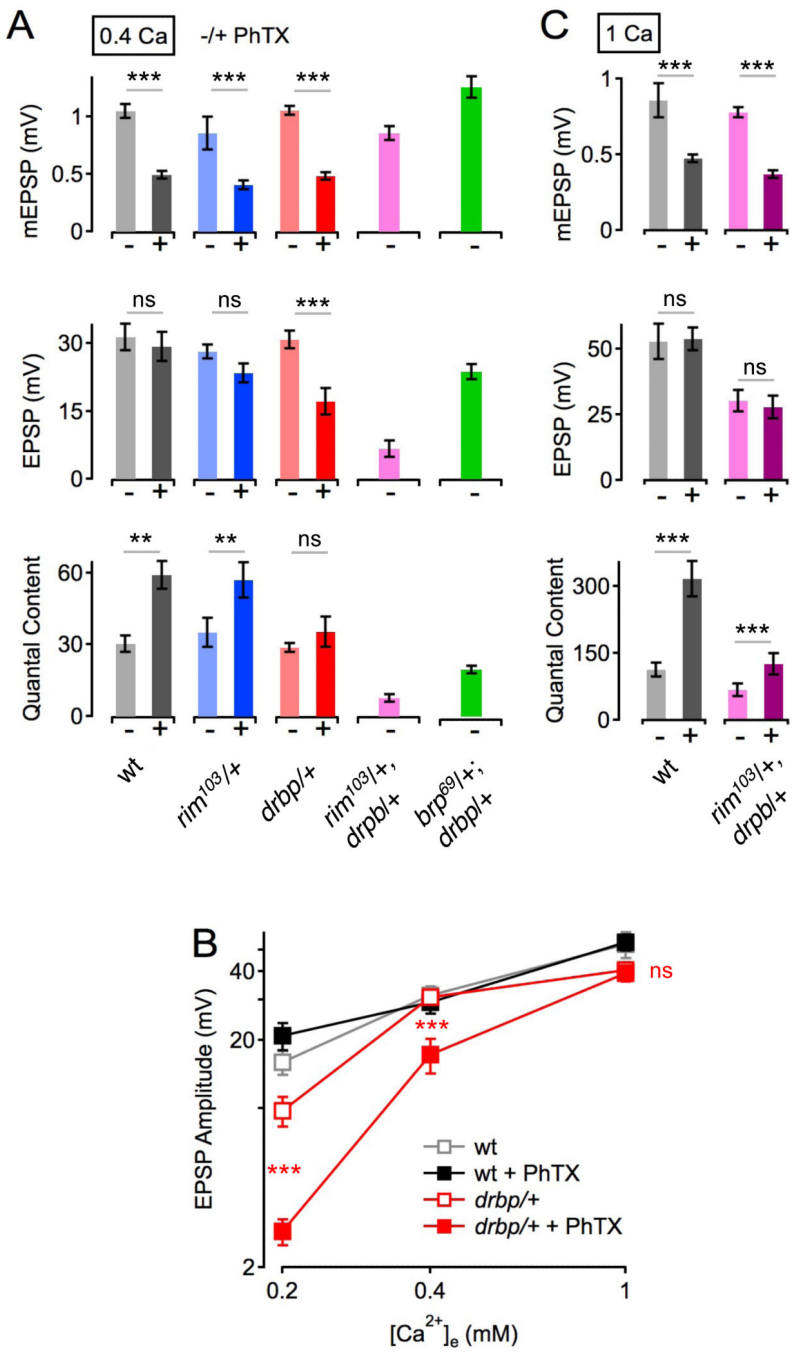

Figure 8. Genetic Interaction between *drbp* and *rim* during Baseline Synaptic Transmission

(A) Average data for mEPSP amplitude (top), EPSP amplitude (middle) and quantal content (bottom) in the absence (−) and presence (+) of PhTX for the genotypes indicated at the bottom (0.4 mM $[Ca^{2+}]_e$). wt (−PhTX): n=6; wt (+PhTX): n=6; *rim103/+* (−PhTX): n=7; *rim103/+* (+PhTX): n=5; *drbp/+* (−PhTX): n=10; *drbp/+* (+PhTX): n=19; *rim103/drbp* (−PhTX): n=12; brp^{69}*/+;drbp/+* (−PhTX): n=10.

(B) Average EPSP amplitudes in the absence and presence of PhTX as a function of $[Ca^{2+}]_e$ of the indicated genotypes (0.2mM $[Ca^{2+}]_e$: wt (−PhTX): n=8; wt (+PhTX): n=8; *drbp/+*

(−PhTX): n=16; *drbp/+* (+PhTX): n=16; 1mM $[Ca^{2+}]_e$: wt (−PhTX): n=6; wt (+PhTX): n=6; *drbp/+* (−PhTX): n=12; *drbp/+* (+PhTX): n=12; 0.4mM $[Ca^{2+}]_e$ as in (A)). Note the significant decrease in EPSP amplitude in *drbp/+* following PhTX treatment at the two lowest $[Ca^{2+}]_e$ with respect to baseline conditions (all $p<0.001$), and the decrease in EPSP amplitude in *drbp/+* in the absence of PhTX at 0.2mM $[Ca^{2+}]_e$ compared to wild type ($p=0.019$).

(C) Average data for mEPSP amplitude (top), EPSP amplitude (middle) and quantal content (bottom) in the absence (−) and presence (+) of PhTX for the genotypes at 1mM $[Ca^{2+}]_e$ (*rim*^{103}*/drbp* (−PhTX): n=12; *rim*^{103}*/drbp* (+PhTX): n=12; n for wild type are given in (B)).

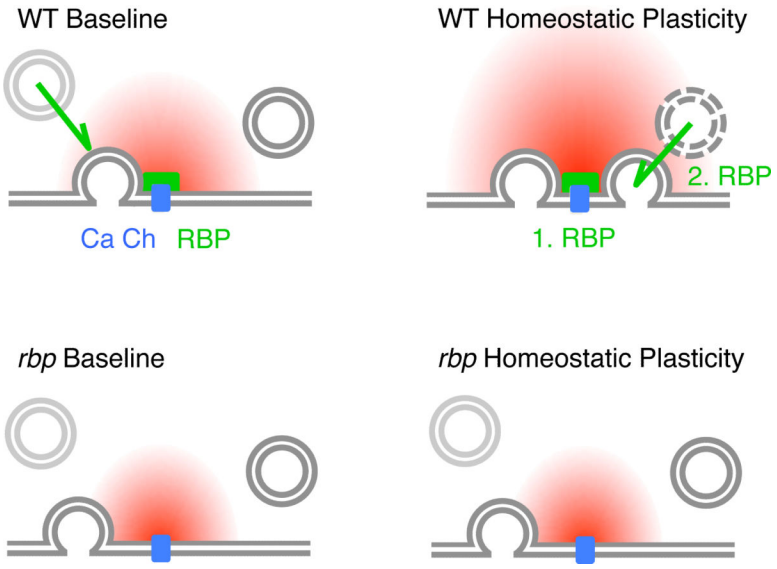

Figure 9. Model for RBP's Role in Homeostatic Plasticity and Vesicle Resupply

Our data suggest that RBP (green), which is located in close proximity to voltage-gated Ca^{2+} channels ('Ca Ch', blue) (Liu et al., 2011), is necessary for both, the homeostatic enhancement of presynaptic Ca^{2+} influx ('1. RBP') and for the homeostatic increase in the number of release-ready vesicles ('2. RBP'). Under baseline conditions, RBP is required for 'tight coupling' between vesicles and Ca^{2+} channels (note the increased distance between vesicle and Ca^{2+} channel in *rbp*), normal levels of presynaptic Ca^{2+} influx (decreased Ca^{2+} domain size in *rbp*) (Liu et al., 2011), and for the rapid resupply of 'fast' release-ready vesicles (green arrow).